Capillary flow enhancement in rectangular polymer microchannels with a deformable wall

R. Anoop and A. K. Sen
Department of Mechanical Engineering, Indian Institute of Technology Madras, Chennai 600036, India
(Received 11 June 2015; published 31 July 2015)

We report the capillary flow enhancement in rectangular polymer microchannels, when one of the channel walls is a deformable polymer membrane. We provide detailed insight into the physics of elastocapillary interaction between the capillary flow and elastic membrane, which leads to significant improvements in capillary flow performance. As liquid flows by capillary action in such channels, the deformable wall deflects inwards due to the Young-Laplace pressure drop across the liquid meniscus. This, in turn, decreases the radius of curvature of the meniscus and increases the driving capillary pressure. A theoretical model is proposed to predict the resultant increase in filling speed and rise height, respectively, in deformable horizontal and vertical microchannels having large aspect ratios. A non-dimensional parameter J, which represents the ratio of the capillary force to the mechanical restoring force, is identified to quantify the elastocapillary effects in terms of the improvement in filling speed (for $J > 0.238$) and the condition for channel collapse ($J > 1$). The theoretical predictions show good agreement with experimental data obtained using deformable rectangular poly(dimethylsiloxane) microchannels. Both model predictions and experimental data show that over 15% improvement in the Washburn coefficient in horizontal channels, and over 30% improvement in capillary rise height in vertical channels, are possible prior to channel collapse. The proposed technique of using deformable membranes as channel walls is a viable method for capillary flow enhancement in microfluidic devices.

DOI: 10.1103/PhysRevE.92.013024 PACS number(s): 47.61.−k

I. INTRODUCTION

Surface tension forces can have significant influence on liquid flow at micrometer length scales typically encountered in microfluidic devices. The ingress of liquid into fine tubes and porous solids, and the rise of liquids in vertical capillary tubes, are common examples of flows driven by surface tension. The capillary action of liquids can be used as a passive method of driving fluid flow in microfluidic devices, without external pumps or actuators [1], and the dynamics of capillary flow in rigid horizontal channels and vertical tubes is well investigated in literature [2–4]. Surface tension and capillary pressure difference across menisci can also be sufficiently strong to deform elastic microstructures; such elastocapillary mechanisms are responsible for the coalescence of wet hair [5], tarsal adhesion that helps beetles cling strongly to surfaces [6], the stiction, collapse, and sometimes failure of flexible micromachined structures after wet-etching process [7], and the collapse of liquid-filled carbon nanotubes [8] and deformable microchannels [9]. The elastocapillary rise of liquids between parallel walls, one or both of which are flexible, has been reported and studied in literature [10]. Elastocapillary interactions can also cause buckling and collapse in flexible tubes dipped vertically into a wetting liquid [11]. Elastocapillary filling of silicon nanochannels was studied using a simple model and experiments [9]. However, the model provided limited theoretical insight into the fundamental physical mechanisms that underly the elastocapillary interaction; it does not predict the conditions for improvement in filling speed or channel collapse, which are critical in fully contemplating the process.

Here we attempt to derive, from first principles, a detailed theoretical model for the capillary filling of deformable horizontal microchannels, and extend the theory to predict capillary rise height in deformable vertical microchannels. The liquid advancing in a rectangular microchannel by capillary action is below ambient pressure due to the capillary pressure drop across the curved liquid meniscus. If one of the channel walls is deformable, it deflects inwards due to the difference in pressure between the liquid within the channel and the ambient air outside. This decreases the radius of curvature of the meniscus and, in accordance to the Young-Laplace equation, increases the driving capillary pressure; consequently, capillary flow in a deformable channel is improved in comparison to a rigid channel. We show that the effect of wall compliance on capillary flow is fully quantified by a non-dimensional parameter J that represents the ratio of surface tension to wall rigidity. The theoretical results are then validated using experimental data obtained from microchannels fabricated in polydimethylsiloxane (PDMS) polymer.

II. THEORETICAL MODEL

A. Deflection of the compliant wall

We consider a thin, rectangular polymer membrane of width w, length L, and thickness t, forming one wall of a rectangular microchannel as shown in Fig. 1(a). Let E and ν denote, respectively, its Young's modulus and Poisson's ratio. The edges $y = \pm w/2$ are considered built in. The liquid (gage) pressure $-p(x)$ acts transversely on the membrane, causing a deflection $\omega(x,y)$. Assuming the pure bending theory for thin plates gives a reasonable approximation to the actual deflection, we write

$$\frac{\partial^4\omega}{\partial x^4} + 2\frac{\partial^4\omega}{\partial x^2\partial y^2} + \frac{\partial^4\omega}{\partial y^4} = -\frac{p(x)}{D}, \tag{1}$$

where $D = Et^3/12(1-\nu^2)$ is the flexural rigidity of the membrane [12]. To non-dimensionalize the equation, we set $x' = x/L$, $y' = y/w$, $\omega' = \omega/\hat{\delta}$ and $p'(x') = p(x)w^4/\hat{\delta}D$, $\hat{\delta}$ being the maximum membrane deflection. The non-dimensional

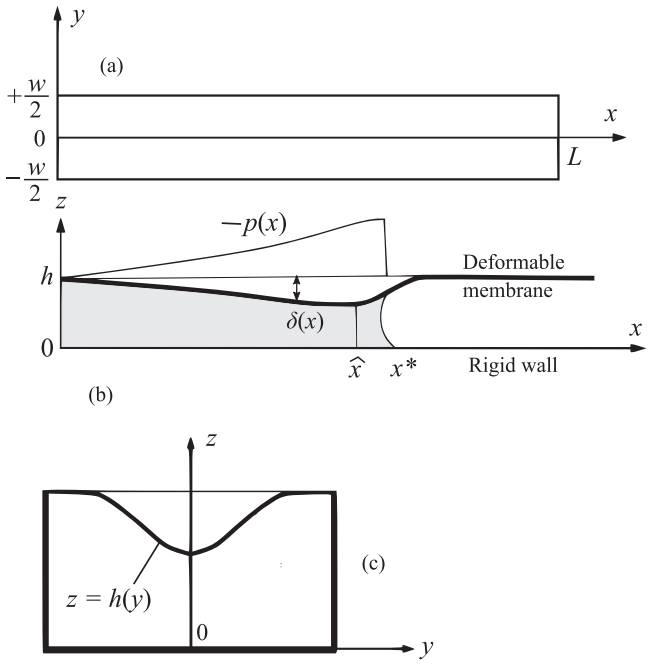

FIG. 1. Capillary flow in a deformable channel and the coordinate system used for theoretical analysis. (a) Top view of deformable membrane wall; (b) Side view of liquid advancing in a deformable channel, and deflection profile of the membrane wall; and (c) Cross sectional view of deformed channel.

form (with primes dropped for clarity) reads

$$\epsilon^4\frac{\partial^4\omega}{\partial x^4}+2\epsilon^2\frac{\partial^4\omega}{\partial x^2\partial y^2}+\frac{\partial^4\omega}{\partial y^4}=-p(x). \tag{2}$$

In the above equation, $\epsilon = w/L$ is the ratio of membrane width to channel length, and is usually much less than 1. We may therefore neglect the terms involving ϵ^4 and ϵ^2, provided the deflection varies gradually with x and y. Integration of this simplified equation, with appropriate boundary conditions at the built-in edges, yields the deflection profile

$$\omega(x,y)=\delta(x)\left[4\left(\frac{y}{w}\right)^2-1\right]^2, \tag{3}$$

where

$$\delta(x)=\omega(x,0)=-\frac{\alpha p(x)w^4}{D} \tag{4}$$

is the maximum deflection at a given x, which occurs at the centerline $y = 0$. The constant α determines the magnitude of deflection and has the value $1/384$.

The pressure $-p(x)$ acting on the membrane is maximum just behind the meniscus, and decreases in magnitude further upstream along the channel. Downstream of the meniscus, the channel is yet to be filled by the liquid and is occupied by air at ambient pressure. Across the meniscus, therefore, the net load impressed on the membrane drops to zero. The maximum deflection $\hat{\delta}$ occurs at a location $x = \hat{x}$, a short distance behind the meniscus at $x = x^*$, as shown in Fig. 1(b). Beyond $\hat{x}$, the membrane quickly relaxes back to zero deflection and Eq. (4) is not valid for $x > \hat{x}$. The deflection at the meniscus δ^* is consequently less than the maximum deflection $\hat{\delta}$; our numerical simulations of membrane deflection showed that $\delta^* = \hat{\delta}/2$ to a very good approximation, in agreement with the assumption in [9]. Further, the change in liquid pressure over the short distance from $\hat{x}$ to x^* is neglected, so that $p(x^*) = p(\hat{x}) = -p_0$.

B. Capillary pressure in a deformed channel

The deflection of the membrane wall reduces the radius of curvature of the liquid meniscus and increases the Young-Laplace pressure drop across the liquid-air interface. Let w and h denote the width and height of the undeformed channel cross section. Due to membrane deflection, the height at the center of the channel at the meniscus is reduced from h to $h - \delta^*$. We approximate the increased pressure drop across the meniscus by

$$p_0=2\sigma\cos\theta\left(\frac{1}{w}+\frac{1}{h-\delta^*}\right), \tag{5}$$

where σ and θ are, respectively, the surface tension of the wetting liquid and its contact angle with the channel walls. Let $a = w/h$ be the aspect ratio of the channel, and $\xi^* = \delta^*/h$ be the non-dimensional deflection at the meniscus. For large aspect ratio channels, $(1/a) << 1$ and hence

$$p_0=\frac{2\sigma\cos\theta}{h}\left(\frac{1}{a}+\frac{1}{1-\xi^*}\right)\approx\frac{2\sigma\cos\theta}{h(1-\xi^*)}. \tag{6}$$

From Eq. (4),

$$p_0=-p(\hat{x})=\frac{\hat{\delta}D}{\alpha w^4}=\frac{2\delta^*D}{\alpha w^4}=\frac{2\xi^*Dh}{\alpha w^4} \tag{7}$$

since $\hat{\delta} = 2\delta^*$. Equating the two expressions for p_0 gives

$$\hat{\xi}=2\xi^*=1-\sqrt{1-J}, \tag{8}$$

where $\hat{\xi} = \hat{\delta}/h$, and the parameter J is defined as

$$J=\frac{4\alpha w^4\sigma\cos\theta}{Dh^2}, \tag{9}$$

The non-dimensional parameter J represents the ratio of the capillary force $2a\sigma\cos\theta\,\mathrm{d}x$ to the mechanical restoring force at 50% membrane deflection $(D/2\alpha a w^2)\,\mathrm{d}x$. For $J > 1$, there is no real solution for ξ^*; the membrane in this case is too compliant and collapses under capillary pressure. If we define the elastocapillary length λ as $\sqrt{D/\sigma\cos\theta}$ [13], then J can be expressed in terms of the ratio h/λ and the aspect ratio a as $J = 4\alpha a^4(h/\lambda)^2$. Henceforth, we find that the effects of wall compliance appear in theoretical expressions solely in terms of the parameter J.

C. Flow resistance of the deformed channel

The inward deflection of the membrane increases the viscous pressure loss in the deformed channel. Consider the cross section at an arbitrary point x, as shown in Fig. 1(c); we assume the velocity profile $\mathbf{v} = u(y,z)\mathbf{e}_x$ to be fully developed and the pressure $p(x)$ to be constant at this section, and use the Poiseuille equation,

$$\mu\left(\frac{\partial^2u}{\partial y^2}+\frac{\partial^2u}{\partial z^2}\right)=\frac{\partial p}{\partial x}, \tag{10}$$

where μ is the dynamic viscosity of the (Newtonian) liquid [14]. If Q is the total volumetric flow rate, $U_0 = Q/wh$ gives a suitable velocity scale for the problem. We change variables to $Y = y/w$, $Z = z/h$ and $U = u/U_0$, and get

$$\frac{1}{a^2}\frac{\partial^2 U}{\partial Y^2} + \frac{\partial^2 U}{\partial Z^2} = \frac{wh^3}{\mu Q}\frac{\partial p}{\partial x} = P \text{ (constant)}. \tag{11}$$

We restrict ourselves to large aspect ratio channels, and drop the term involving $1/a^2$. From Eq. (3), we see that the height of the channel varies along the width as $H(Y) = 1 - \xi(4Y^2 - 1)^2$, where $H(Y) = h(y)/h$ and $\xi = \delta(x)/h$. Along with no-slip boundary conditions at the bottom ($Z = 0$) and top [$Z = H(Y)$] walls, Eq. (11) yields the velocity profile

$$U(Y,Z) = \tfrac{1}{2}PZ[Z - H(Y)]. \tag{12}$$

The form of non-dimensionalization requires that

$$\iint \mathrm{d}Y\, \mathrm{d}Z\, U(Y,Z) = 1, \tag{13}$$

from which we obtain the hydraulic resistance per unit length of the deformed cross section to be

$$R_{||} = \frac{1}{Q}\left(-\frac{\partial p}{\partial x}\right) = \frac{12\mu}{wh^3}\frac{1}{s(\xi)}, \tag{14}$$

where

$$s(\xi) = 1 - \frac{8\xi}{5} + \frac{128\xi^2}{105} - \frac{1024\xi^3}{3003}. \tag{15}$$

The velocity in Eq. (12) is non-zero at the side walls $Y = \pm 1/2$; Eq. (14) therefore underpredicts the hydraulic resistance. To correct for this inaccuracy, we include the factor $\beta = 1 - (0.630/a)$, as is done in the case of a rectangular channel approximated as two parallel plates [14]:

$$R = \frac{R_{||}}{\beta} = \frac{12\mu}{\beta wh^3}\frac{1}{s(\xi)}. \tag{16}$$

The cross-sectional area of the channel at the meniscus is also reduced; the new area of cross section at the meniscus location is given by $A^* = wh\Gamma$, where

$$\Gamma = \iint 1\, \mathrm{d}Y\, \mathrm{d}Z\,\Big|_{x=x^*} = 1 - \frac{8\xi^*}{15} = 1 - \frac{4\hat{\xi}}{15}. \tag{17}$$

D. Capillary filling of a horizontal channel

Consider a horizontal microchannel with a deformable membrane wall and both ends open to the atmosphere, as shown in Fig. 1(b). If a small quantity of liquid is introduced at one end, the liquid front advances into the channel by capillary action, and continues downstream as long as channel length is available for wetting. For simplicity, we assume the flow to be quasi-steady and fully developed at all instants of time. Neglecting entrance losses, $p(x = 0) = 0$, where $x = 0$ at the channel inlet. Differentiating Eq. (4) gives

$$-\frac{\mathrm{d}p}{\mathrm{d}x} = \frac{Dh}{\alpha w^4}\frac{\mathrm{d}\xi}{\mathrm{d}x}, \tag{18}$$

for $0 \leqslant x \leqslant \hat{x}$. From Eq. (16), we also have

$$-\frac{\mathrm{d}p}{\mathrm{d}x} = RQ(t) = \frac{12\mu}{\beta wh^3}\frac{Q(t)}{s(\xi)}, \tag{19}$$

$Q(t)$ being the instantaneous flow rate. We equate the two and integrate [15] from $x = 0$ to $\hat{x}$ and get

$$\frac{12\alpha\mu w^3}{\beta Dh^4}Q(t)\,\hat{x}(t) = S, \tag{20}$$

where

$$S = \hat{\xi}\left(1 - \frac{4\hat{\xi}}{5} + \frac{128\hat{\xi}^2}{315} - \frac{256\hat{\xi}^3}{3003}\right). \tag{21}$$

We now write

$$Q(t) = A^*\frac{\mathrm{d}}{\mathrm{d}t}x^*(t) \approx A^*\frac{\mathrm{d}}{\mathrm{d}t}\hat{x}(t) \tag{22}$$

and use this in Eq. (20) to get

$$\hat{x}\frac{\mathrm{d}\hat{x}}{\mathrm{d}t} = \frac{W_d^2}{2}, \tag{23}$$

where the "modified" Washburn coefficient W_d for a deformable channel is given by

$$W_d = \sqrt{\frac{\beta S Dh^3}{6\alpha\Gamma\mu w^4}}. \tag{24}$$

Let $\hat{x} = 0$ at $t = t_0$. Equation (23) on integration gives

$$x^*(t) = W_d\sqrt{t - t_0}, \tag{25}$$

where we have taken $x^* \approx \hat{x}$. We thus recover the Lucas-Washburn behavior [2,16] as in the case of a rigid channel, but with a different value of the Washburn coefficient. For a rigid rectangular channel, the Washburn coefficient can be shown to be given by

$$W_r = \sqrt{\frac{h\beta\sigma\cos\theta}{3\mu}}, \tag{26}$$

as derived in sources such as [14,16]. Therefore, we get

$$\frac{W_d}{W_r} = \sqrt{\frac{2S}{J\Gamma}}. \tag{27}$$

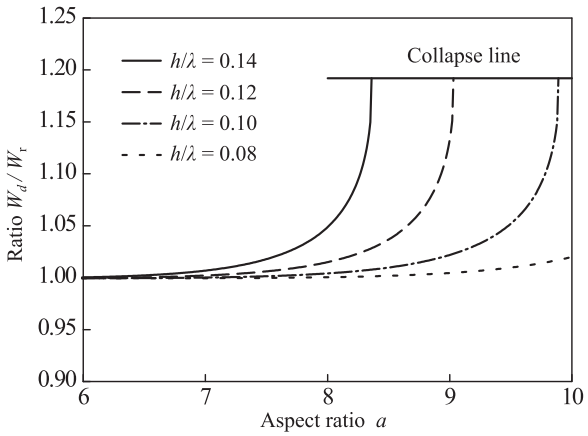

FIG. 2. Theoretical curves for W_d/W_r as a function of a and different values of h/λ, computed from Eq. (27); the collapse line corresponds to $J = 1$ at which W_d/W_r attains a maximum value of 1.192.

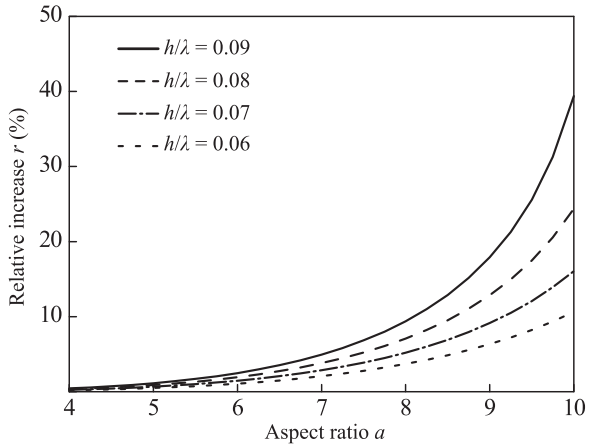

FIG. 3. Relative improvement in rise height r as a function of a and different values of h/λ, as predicted by Eq. (30).

The capillary filling speed is improved due to the presence of the compliant membrane wall if $W_d/W_r > 1$; using Eq. (8), this translates to the condition $J > 0.238$. We also observe that W_d/W_r attains a maximum of 1.192 at $J = 1$, which corresponds to a 19.2% increase in the Washburn coefficient over that of a rigid channel. The value of W_d/W_r, as predicted by Eq. (27), is plotted Fig. 2 as a function of the aspect ratio a for four different values of h/λ.

E. Capillary rise in a vertical channel

Now consider a microchannel held vertically with its lower end dipped in a sump of wetting liquid, and its upper end open to ambient air. The liquid will rise in the channel by capillary action until hydrostatic equilibrium is attained at a finite height above the liquid level in the reservoir. In a deformable channel, the capillary pressure, and hence the rise height, increases due to the deflection of the membrane wall. Let x_r^* and x^* be, respectively, the rise height (measured from the free liquid surface) of the same liquid in rigid and deformable channels of identical dimensions. Then from Eq. (5), we can write

$$r = \frac{x^* - x_r^*}{x_r^*} = \left(\frac{1}{h-\delta^*} - \frac{1}{h}\right) \Big/ \left(\frac{1}{w} + \frac{1}{h}\right) \tag{28}$$

since the rise height is proportional to the capillary pressure drop across the meniscus. Simplifying, we get

$$r = \frac{a}{1+a}\frac{\xi^*}{1-\xi^*}. \tag{29}$$

Using Eq. (8) gives

$$r = \frac{a}{1+a}\left(\frac{1-\sqrt{1-J}}{1+\sqrt{1-J}}\right). \tag{30}$$

The relative improvement r in rise height, as given by the above equation, is plotted in Fig. 3 as a function of the aspect ratio a, for four different values of the ratio h/λ.

III. EXPERIMENTAL RESULTS

For experimental studies, straight rectangular microchannels were fabricated in PDMS polymer (Sylgard 184, Dow Corning) by conventional soft lithography process [17]. Thin membranes were made by spin coating the prepolymer on a plexiglass backing plate and baking in an oven; these were later bonded to the channels after oxygen-plasma exposure to form the compliant wall. The channels so obtained had a uniform rectangular cross section of height 0.1 mm, width in the range of 0.6 mm to 1.3 mm, and a deformable membrane wall 30–40 μm thick, as seen in Fig. 4(a). They were used at least 6 to 8 h after the plasma bonding process, to allow time for the wall surface properties to stabilize.

To measure the filling speed of liquids in horizontal channels, the device was mounted horizontally on the stage of an inverted light microscope (Axio Vert. A1, Zeiss) and a drop of the wetting liquid, about 0.1 mL, was placed on the inlet port using a micropipette. As the liquid filled the channel, the motion of the meniscus was recorded using an attached high-speed camera (Photron Fastcam SA3). The meniscus location x^* as a function of time t was obtained by post-processing the recorded video; the error in position and time measurements were, respectively, ± 0.250 mm and ± 0.004 s. The Washburn coefficient W_f was subsequently computed by fitting Eq. (25) to the data using least-squares method. For measuring the rise height in vertical channels, the devices were kept vertically with the lower end dipped into a petri dish containing the wetting liquid. The meniscus position and the free liquid surface in the reservoir were then photographed against the scale engraved beside the channel,

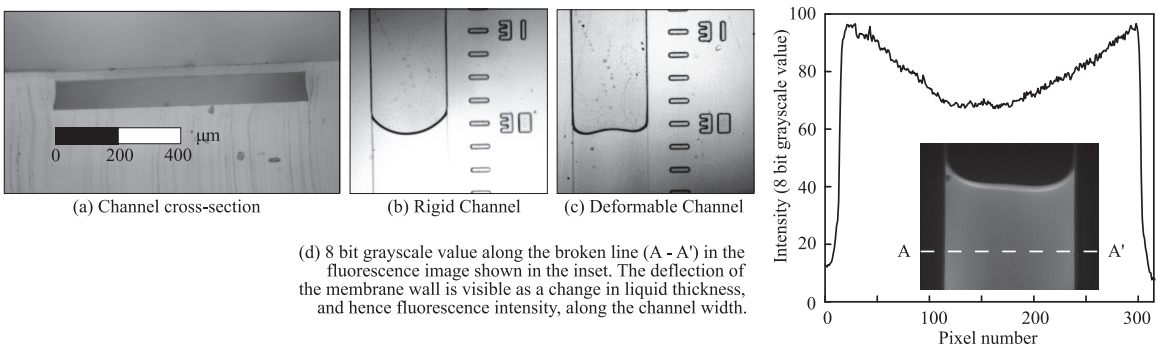

(a) Channel cross-section (b) Rigid Channel (c) Deformable Channel

(d) 8 bit grayscale value along the broken line (A - A') in the fluorescence image shown in the inset. The deflection of the membrane wall is visible as a change in liquid thickness, and hence fluorescence intensity, along the channel width.

FIG. 4. (a) Optical micrograph of the cross section of a deformable channel fabricated in PDMS, measuring 0.790 mm × 0.093 mm with a 0.031 mm membrane wall. (b) and (c) Meniscus shape in identical rigid and deformable channels. (d) Fluorescence micrograph and intensity data showing membrane deflection.

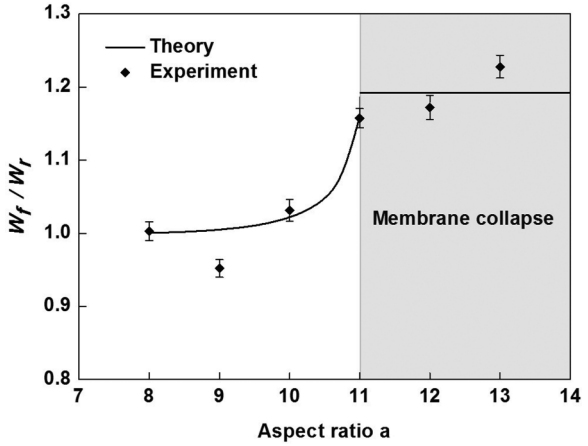

FIG. 5. Experimental (filled diamonds with error bars) and theoretical (solid line) values of W_d/W_r for the filling of propan-2-ol in horizontal deformable microchannels of height 0.1 mm, and various aspect ratios. The theoretical curve and the experimental data agree, with $h/\lambda = 0.0808$; membrane collapse is predicted for $a > 11.01$.

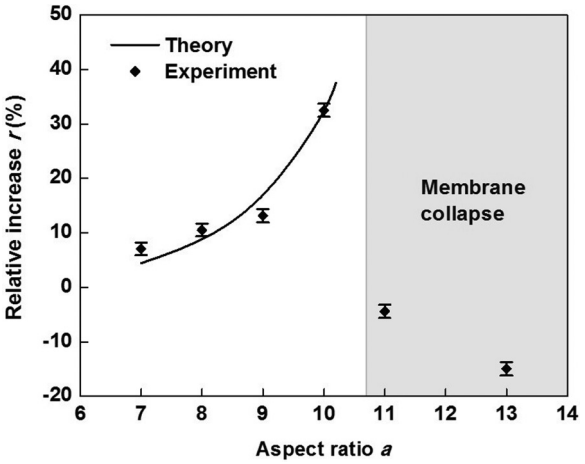

FIG. 6. Experimental (filled diamonds with error bars) and theoretical (solid line) relative increase in capillary rise height r of propane-1,2-diol in vertical deformable microchannels. The theoretical curve closely follows the experimental data with $h/\lambda = 0.0856$, and membrane collapse is predicted for $a > 10.7$.

using a USB microscope (Dino-Lite AM4113ZT); the rise height was found as the difference between these two liquid levels, to within an error of ± 0.500 mm. The measurements were made about 30 min after the channel was lowered into the liquid, to allow adequate time for the liquid meniscus to reach its equilibrium height.

An increase in Washburn coefficient (over the theoretically expected value in an identical rigid channel) was observed in deformable horizontal channels, reaching $(15.7 \pm 1.3)\%$ at an aspect ratio of 11. From Fig. 5, we see that Eq. (27) correctly predicts the increase in W_d/W_r; in particular, the theoretical model gives a maximum increase of 19.2% at $J = 1$, which is well supported by experimental observations. The inward deflection of the compliant wall was separately confirmed by analyzing fluorescence micrographs of a dye solution (Rhodamine B in propan-2-ol) filling the deformable channels [18]. The channel height, and hence the height of the liquid layer within, varies along the width of the channel as a result of the wall deflection; the fluorescence intensity varies proportionately along the channel width, as seen in Fig. 4(d). The inward deflection of the membrane also causes the meniscus to present a concave-convex profile when viewed from above, with a central liquid "finger" [19]; the difference in meniscus shape in rigid and deformable channels was clearly visible during experiments, as seen in Figs. 4(b) and 4(c).

The capillary rise height in vertical deformable channels also showed significant improvement in comparison to the theoretically expected value in rigid channels of identical dimensions, approaching $(32.5 \pm 1.2)\%$ at an aspect ratio of 10. The relative increase r in rise height agrees well with Eq. (30), as seen in Fig. 6. The channels with $a = 11$ and 13 provided negative values of r; during experiments, the membrane wall of these channels had visibly collapsed. We believe that the negative value of r post-collapse is because the liquid rises extremely slowly due to the very high flow resistance of the collapsed channel; the meniscus might not have attained equilibrium even after 30 min, when the measurements were made.

IV. CONCLUSION

The theoretical model presented above provides a detailed insight into the fundamental physics of elastocapillary flow in deformable microchannels. The liquid advancing by capillary action is below ambient pressure due to the Young-Laplace pressure drop across the liquid meniscus. The inward deflection of the deformable wall, caused by this pressure difference, reduces the radius of curvature of the meniscus and increases the driving capillary pressure, thereby improving the filling speed and rise height in deformable microchannels. The non-dimensional parameter J, defined in Eq. (9), appears as a significant parameter in quantifying this elastocapillary interaction in channels of large aspect ratios; the conditions for wall collapse and improvement in filling speed were seen to be, respectively, $J > 1$ and $J > 0.238$. The parameter J is itself a function of the non-dimensional ratios h/λ and $a = w/h$; consequently, the relative increase in the Washburn coefficient and rise height in deformable channels depends solely on these two variables. In a deformable horizontal channel, the maximum value of the Washburn coefficient, which occurs just prior to membrane collapse, is seen to be 1.192 times the value in an identical, rigid channel, which represents a 19.2% improvement in filling speed. The theoretical predictions are in good agreement with experimental results obtained from PDMS microchannels; improvements of over 15% and 30%, respectively, in filling speed and rise height were predicted in deformable channels prior to collapse, and verified using experiments. These results clearly indicate that the technique of using compliant membranes as channel walls is indeed a viable method of enhancing capillary flow in passive microfluidic devices, including "lab on a chip" or μ-TAS devices where faster response and reduced cycle times are desired.

ACKNOWLEDGMENTS

This work was supported by the Indian Institute of Technology Madras via project no. ERP 1314018 RESFASHS.

[1] D. Juncker, H. Schmid, U. Drechsler, H. Wolf, M. Wolf, B. Michel, N. de Rooij, and E. Delamarche, Anal. Chem. **74**, 6139 (2002); R. Safavieh and D. Juncker, Lab Chip **13**, 4180 (2013); M. Zimmermann, H. Schmid, P. Hunziker, and E. Delamarche, *ibid.* **7**, 119 (2007).

[2] E. W. Washburn, Phys. Rev. **17**, 273 (1921).

[3] Y. Zhu and K. Petkovic-Duran, Microfluid. Nanofluid. **8**, 275 (2010); Y. Xiao, F. Yang, and R. Pitchumani, J. Colloid Interface Sci. **298**, 880 (2006).

[4] M. Stange, M. E. Dryer, and H. J. Rath, Phys. Fluids **15**, 2587 (2003).

[5] J. Bico, B. Roman, L. Moulin, and A. Boudaoud, Nature **432**, 690 (2004).

[6] T. Eisner and D. J. Aneshansley, Proc. Nat. Acad. Sci. USA **97**, 6568 (2000).

[7] C. H. Mastrangelo and C. H. Hsu, J. Microelectromech. Syst. **2**, 44 (1993).

[8] Y. Yang, Y. F. Gao, D. Y. Sun, M. Asta, and J. J. Hoyt, Phys. Rev. B **81**, 241407 (2010).

[9] J. W. van Honschoten, M. Escalante, N. R. Tas, H. V. Jansen, and M. Elwenspoek, J. Appl. Phys. **101**, 094310 (2007).

[10] H.-Y. Kim and L. Mahadevan, J. Fluid Mech. **548**, 141 (2006); T. Cambau, J. Bico, and E. Reyssat, Europhys. Lett. **96**, 24001 (2011); C. Duprat, J. M. Aristoff, and H. A. Stone, J. Fluid Mech. **679**, 641 (2011).

[11] T. B. Hoberg, E. Verneuil, and A. E. Hosoi, Phys. Fluids **26**, 122103 (2014).

[12] S. Timoshenko and S. Woinowsky-Krieger, *Theory of Plates and Shells*, 2nd ed. (McGraw-Hill Book Company, Inc., New York, 1959).

[13] B. Roman and J. Bico, J. Phys.: Condens. Matter **22**, 493101 (2010).

[14] H. Bruus, *Theoretical Microfluidics* (Oxford University Press, Inc., Oxford, 2008).

[15] In integrating the resistance R over distance x,we consider the channel to consist of a series of infinitesimal segments whose individual resistances can be simply summed. This "lubrication approximation" is acceptable if the deflection varies gradually with x. See, M. Akbari, D. Sinton, and M. Bahrami, Int. J. Heat Mass Transfer **54**, 3970 (2011).

[16] J. W. van Honschoten, N. Brunets, and N. R. Tas, Chem. Soc. Rev. **39**, 1096 (2010).

[17] J. C. McDonald and G. M. Whitesides, Acc. Chem. Res. **35**, 491 (2002); Y. Xia and G. M. Whitesides, Annu. Rev. Mater. Sci. **28**, 153 (1998).

[18] B. S. Hardy, K. Uechi, J. Zhen, and H. P. Kavehpour, Lab Chip **9**, 935 (2009).

[19] J. W. van Honschoten, M. Escalante, N. R. Tas, and M. Elwenspoek, J. Colloid Interface Sci. **329**, 133 (2009).